

Sensitivity of the decay $h \rightarrow ZZ^* \rightarrow Zl + l^-$ to the Higgs self coupling through radiative corrections

H. Castilla-Valdez,^{*} A. Moyotl,[†] and M. A. Perez[‡]

*Departamento de Física, CINVESTAV,
Apartado Postal 14-740, 07000 México, D. F., México.*

C. G. Honorato[§]

*Fac. de Cs. de la Electrónica, Benemérita Universidad Autónoma de Puebla,
Apartado Postal 542, 72570 Puebla, Puebla, México*

(Dated: March 5, 2018)

We study the radiative corrections induced by the triple Higgs boson coupling hhh in the three body decay $h \rightarrow ZZ^* \rightarrow Zl\bar{l}$. We show that these corrections are potentially sensitive to the specific value of this coupling in the Standard Model and the Two Higgs Doublet Model (2HDM). These effects may induce corrections to the integrated decay width of the three-body decay of order few percent in the 2HDM and thus open a new window to test the Higgs boson self interaction in physics beyond the standard model. .

PACS numbers: 14.80.Ec, 12.60.Fr, 14.70.Hp

I. INTRODUCTION

The accumulated data at the LHC has confirmed that the new particle with a mass of about 125 GeV corresponds to the state responsible for the electroweak symmetry breaking mechanism of the Standard Model (SM) [1, 2]. This data indicates also that the couplings of this state to fermions and gauge bosons are consistent with those expected in the SM for the Higgs boson [3]. An immediate task now is to measure the Higgs self-coupling hhh which

^{*}Electronic address: castilla@fis.cinvestav.mx

[†]Electronic address: amoyotl@fis.cinvestav.mx

[‡]Electronic address: mperez@fis.cinvestav.mx

[§]Electronic address: carlosg.honorato@correo.buap.mx

will determine the structure of the Higgs potential in the SM. Measuring this coupling will be then an important step to conclude that the observed scalar boson [1, 2] is identical to the Higgs boson predicted by the SM.

It has been pointed out that the hhh coupling may be accessible in the double Higgs production in both e^+e^- linear colliders [4, 5] and at the LHC [6, 7]. However, the production cross section in the latter case is about two orders of magnitude below the single Higgs production case [8]. The gluon-gluon (GGF) and vector boson fusion (VBF) modes seem to be the most sensitive channels to the hhh contribution for the double Higgs production process [9–11]. Unfortunately, the respective cross sections for these modes have to be measured with an accuracy of about 50% at $\sqrt{s} = 8 \text{ TeV}$ in order to be able to extract the trilinear coupling with a similar accuracy [9]. The situation may be improved at a 100 TeV hadron collider with a $bb\gamma\gamma$ final state [12]. On the other hand, it has been pointed out that a precise measurement of the ratio of cross sections of the double-to-single Higgs boson production at the LHC may become the most precise method for determination of the Higgs trilinear coupling [13]. However, it is not clear if a meaningful measurement of the Higgs self-coupling at the LHC is possible due to the relative high uncertainties on the HH cross sections measurements in both CMS and ATLAS [14].

It has been known that indirect tests of new physics effects can be performed by precision measurements of observables sensitive to radiative corrections [15]. In particular, the study of deviations of the Higgs boson couplings from the SM predictions may discriminate among various new physics models. The measurement accuracy of these coupling constants will be improved at future experiments such as the High Luminosity LHC (HL-LHC), and even most of the Higgs couplings are expected to be measured with typically of 10% or better accuracy [16–18]. In the present paper we are interested in testing if the trilinear self-coupling of the Higgs boson may be detected through its virtual effects in the radiative corrections to the decay mode $h \rightarrow ZZ^* \rightarrow Zl^+l^-$. We will obtain that these corrections are potentially sensitive to the specific value of the Higgs self-coupling in the SM and in the 2HDM. The one-loop effects for the hZZ coupling has been computed in the SM [18], the 2HDM [16] and the Inert Higgs Doublet Model (IHDM) [19]. In all these cases, the radiative corrections are small between 1% and 2%. However, we will show that variations on the hhh coupling may induce higher corrections on the partial decay width of $h \rightarrow ZZ^* \rightarrow Zl^+l^-$ and thus open a window to test the self Higgs coupling if the respective decay width can be measured

with an accuracy of order 4%. Deviations of the triple self coupling with respect to the SM predictions has been observed in the effective Lagrangian framework 2HDM [16] and in radiative corrections in 2HDM [20, 21].

The plan of the paper is as follows. In Section II we present the details of the radiative corrections to one-loop order of the decay width for $h \rightarrow ZZ^* \rightarrow Zl^+l^-$ in the SM; section III contains the respective calculation for the the 2HDM. Conclusions are given in Section IV while the Appendix includes the definitions for the different structure functions used in our calculation.

II. SM FRAMEWORK

This decay process occurs, at first glance, in the SM context. Actually, it is achieved at tree level, but the relevant effects due the hhh vertex, are induced at one loop level. With the general aim to present a clear analysis over de Higgs potential we will use the following notation

$$V_h = \mu^2 \Phi \Phi^\dagger + \frac{1}{2} \lambda (\Phi \Phi^\dagger)^2, \quad (1)$$

with Φ the Higgs doublet and after the EWSB with v the vacuum expectation value the Higgs potential takes the expression

$$V_h = \frac{1}{2} m_h^2 h^2 + \lambda_{3h} v (h)^3 + \frac{1}{4} \lambda_{4h} h^4, \quad (2)$$

with $\lambda_{3h} = \frac{m_h^2}{2v^2}$ and $\lambda_{4h} = \lambda_{3h}$ in the SM. For a Higgs mass of 125 GeV and $v = 248$ GeV we get $\lambda_{3h} = 0.13$. We will find convenient to use a normalized Higgs self coupling [8]:

$$\lambda = \frac{\lambda_{NP}}{\lambda_{SM}}. \quad (3)$$

The Higgs decay $h \rightarrow ZZ^* \rightarrow Zl^+l^-$ proceeds through the Feynman diagram shown in Figure 1. The black vertex represents all the perturbative contributions that are included in Figures 2-5 to one-loop order. The integrated decay width is given by [22]:

$$\Gamma(h_{SM} \rightarrow Zll) = \frac{m_h}{256\pi^3} \int_{x_{1i}}^{x_{1f}} \int_{x_{2i}}^{x_{2f}} |\bar{\mathcal{M}}|^2 dx_2 dx_1, \quad (4)$$

with the kinematical invariant variables

$$s_1 = (p_Z + p_1)^2 = (p - p_2)^2, \quad (5)$$

$$s_2 = (p_1 + p_2)^2 = (p - p_Z)^2, \quad (6)$$

$$s_3 = (p_2 + p_Z)^2 = (p - p_1)^2, \quad (7)$$

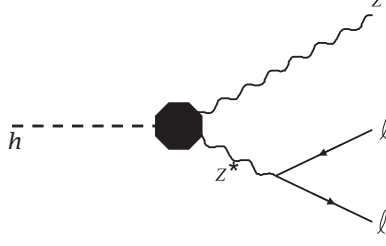


FIG. 1: Feynman diagram for decay $h \rightarrow ZZ^* \rightarrow Zll$.

p_Z , p and p_i ($i = 1, 2$) correspond to the four momenta of the emitted Z gauge bosons, the Higgs boson and the two leptons in the final state, and the integration limits are given by:

$$x_{1i} = 2\sqrt{\xi_Z}, \quad (8)$$

$$x_{1f} = 1 + \xi_Z - 4\xi_l, \quad (9)$$

$$x_{2i} = \frac{2 - x_1}{2} + \frac{\sqrt{(x_1^2 - 4\xi_Z)(x_1 - 1 + 4\xi_l - \xi_Z)}}{2\sqrt{x_1 - \xi_Z - 1}}, \quad (10)$$

$$x_{2f} = \frac{2 - x_1}{2} - \frac{\sqrt{(x_1^2 - 4\xi_Z)(x_1 - 1 + 4\xi_l - \xi_Z)}}{2\sqrt{x_1 - \xi_Z - 1}}, \quad (11)$$

with $\xi_Z = m_Z^2/m_h^2$, $\xi_l = m_l^2/m_h^2$, $s_1 = m_h^2(-1 + x_1 + x_2 + \xi_l)$ and $s_2 = m_h^2(1 - x_1 + \xi_Z)$. The square of invariant amplitude given in Eq.(4) will be expressed in terms of the hZZ^* effective and Zff vertices,

$$g_{hZZ}^{\alpha\beta} = \frac{igm_Z}{c_W} \left(\mathcal{G}_0 g^{\alpha\beta} + \mathcal{G}_1 \left[\mathcal{F}^g g^{\alpha\beta} + \mathcal{F}^k k_1^\alpha k_2^\beta \right] \right), \quad (12)$$

$$g_{Zff} = \frac{ig}{4c_W} \gamma^\mu (f_V + \gamma^5 f_A), \quad (13)$$

$$\begin{aligned} |\mathcal{M}|^2 &= \frac{-g^4(f_A^2 + f_V^2)}{8c_W^4 m_Z^4} \left| \mathcal{G}_0 + \mathcal{F}^g \mathcal{G}_1 \right|^2 \frac{1}{(s_2 - m_Z^2)^2} \left\{ 2k_s^4 m_f^2 (2m_Z^2 - s_2) \right. \\ &\quad \left. + m_Z^4 \left[m_f^4 + m_f^2 (m_h^2 + 3m_Z^2 - 2s_1 - s_2) \right. \right. \\ &\quad \left. \left. + (m_h^2 - s_1)(m_Z^2 - s_1) + s_2(s_1 - 2m_Z^2) \right] \right\} \\ &\equiv \frac{-g^4(f_A^2 + f_V^2)}{8c_W^4 m_Z^4} \left| \mathcal{G}_0 + \mathcal{F}^g \mathcal{G}_1 \right|^2 \mathcal{K}(s_1, s_2, m_h, m_Z, m_f), \end{aligned} \quad (14)$$

where we have defined for convenience the function $\mathcal{K}(s_1, s_2, m_h, m_Z, m_f)$ and used the hZZ^* form factors \mathcal{G}_0 , \mathcal{G}_1 , \mathcal{F}^g and \mathcal{F}^k whose expressions are included in Appendix for the SM and the 2HDM. It is important to notice that the form factor \mathcal{F}^k does not contribute to the invariant amplitude given in Eq.(14) because the $Z(p_Z)$ gauge boson is on mass shell.

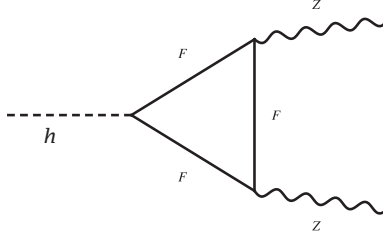


FIG. 2: Generic one-loop fermionic contribution to the hZZ vertex.

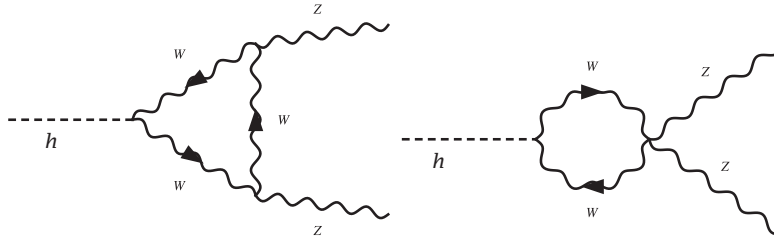


FIG. 3: Pure W -Boson contribution to hZZ vertex.

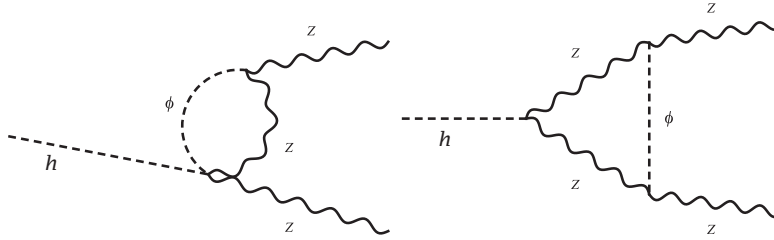


FIG. 4: Scalar contributions to the hZZ vertex that are independent of the hhh coupling. In the SM $\phi = h$ and in 2HDM $\phi = \{h, H\}$.

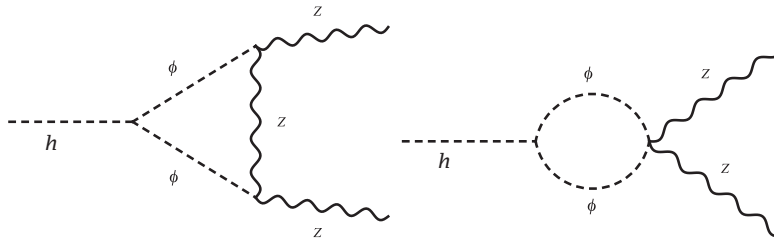


FIG. 5: Scalar contribution to the hZZ vertex that depends on the hhh coupling. In the SM $\phi = h$ and in 2HDM $\phi = \{h, H\}$.

The contributions to the decay width given in Figures 2-5 can be expressed in terms of the tree contribution (with $\mathcal{G}_0 = 1$), the 1-loop term associated to the Feynman diagrams shown in Figures 2-5, and the respective interference term,

$$|\mathcal{M}_{SM}|_{tree}^2 = \frac{-g^4(f_A^2 + f_V^2)}{8c_W^4 m_Z^4} \mathcal{K}(s_1, s_2, m_h, m_Z, m_f). \quad (15)$$

$$\begin{aligned} |\mathcal{M}_{SM}|_{1-loop}^2 &= \frac{-g^4(f_A^2 + f_V^2)\mathcal{G}_1^2 |\mathcal{F}_{SM}^g|^2}{8c_W^4 m_Z^4} \mathcal{K}(s_1, s_2, m_h, m_Z, m_f) \\ &= \frac{-g^4(f_A^2 + f_V^2)}{8c_W^4 m_Z^4} \left(\frac{g^2 c_W}{128\pi^2 k_s^8 m_Z} \right)^2 |\mathcal{F}_{fSM}^g + \mathcal{F}_{WSM}^g + \mathcal{F}_{SSM}^g + \mathcal{F}_{3hSM}^g|^2 \\ &\quad \times \mathcal{K}(s_1, s_2, m_h, m_Z, m_f), \end{aligned} \quad (16)$$

$$\mathcal{F}_{SM}^g = \mathcal{F}_{fSM}^g + \mathcal{F}_{WSM}^g + \mathcal{F}_{SSM}^g + \mathcal{F}_{3hSM}^g, \quad (17)$$

$$\begin{aligned} \mathcal{M}_{int} &= \frac{-g^4(f_A^2 + f_V^2)}{4c_W^4 m_Z^4} \left(\frac{g^2 c_W}{128\pi^2 k_s^8 m_Z} \right) Re[\mathcal{F}_{fSM}^g + \mathcal{F}_{WSM}^g + \mathcal{F}_{SSM}^g + \mathcal{F}_{3hSM}^g] \\ &\quad \times \mathcal{K}(s_1, s_2, m_h, m_Z, m_f). \end{aligned} \quad (18)$$

The explicit expressions for the SM form factors \mathcal{F}_{iSM}^g given in Eqs. (16-18) are included in the Appendix.

The integrated SM decay width takes then the following form

$$\begin{aligned} \Gamma(h_{SM} \rightarrow Zll) &= \frac{m_h}{256\pi^3} \left(\frac{-g^4(f_A^2 + f_V^2)}{8c_W^4 m_Z^4} \right) \int_{x_{1i}}^{x_{1f}} \int_{x_{2i}}^{x_{2f}} \left[1 + \frac{2g^2 c_W}{128\pi^2 k_s^8 m_Z} \right. \\ &\quad \times Re[\mathcal{F}_{fSM}^g + \mathcal{F}_{WSM}^g + \mathcal{F}_{SSM}^g + \mathcal{F}_{3hSM}^g] \\ &\quad \left. + \left(\frac{g^2 c_W}{128\pi^2 k_s^8 m_Z} \right)^2 |\mathcal{F}_{fSM}^g + \mathcal{F}_{WSM}^g + \mathcal{F}_{SSM}^g + \mathcal{F}_{3hSM}^g|^2 \right] \\ &\quad \times \mathcal{K}(s_1, s_2, m_h, m_Z, m_f) dx_2 dx_1. \end{aligned} \quad (19)$$

III. 2HDM FRAMEWORK

The most general Two Higgs Doublet Model (2HDM) potential is given by [23]

$$\begin{aligned} V(\Phi_1, \Phi_2) &= \mu_1^2(\Phi_1^\dagger \Phi_1) + \mu_2^2(\Phi_2^\dagger \Phi_2) - \left(\mu_{12}^2(\Phi_1^\dagger \Phi_2) + H.c. \right) + \lambda_1(\Phi_1^\dagger \Phi_1)^2 \\ &\quad + \lambda_2(\Phi_2^\dagger \Phi_2)^2 + \lambda_3(\Phi_1^\dagger \Phi_1)(\Phi_2^\dagger \Phi_2) + \lambda_4(\Phi_1^\dagger \Phi_2)(\Phi_2^\dagger \Phi_1) \\ &\quad + \frac{1}{2} \left(\lambda_5(\Phi_1^\dagger \Phi_2)^2 + \left(\lambda_6(\Phi_1^\dagger \Phi_1) + \lambda_7(\Phi_2^\dagger \Phi_2) \right) (\Phi_1^\dagger \Phi_2) + H.c. \right), \end{aligned} \quad (20)$$

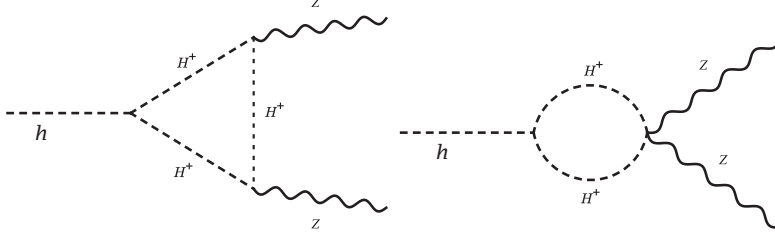


FIG. 6: Higgs charged boson contribution to the hZZ vertex in the 2HDM.

where the two iso-spin Higgs doublets Φ_i , $i = 1, 2$, receive vacuum expectation values v_1 and v_2 , respectively, and have hypercharge +1. We define $\tan\beta = v_2/v_1$ and they satisfy the relation $v(246\text{GeV}) = \sqrt{v_1^2 + v_2^2} = (\sqrt{2}G_F)^{-1/2}$. The parameters μ_{12} , λ_5 , λ_6 and λ_7 are in general complex numbers, but we will set them real in order to maintain CP conservation. A discrete symmetry \mathcal{Z}_2 avoids flavor changing neutral currents. The terms μ_{12} , λ_6 and λ_7 break explicitly this symmetry but we will keep the μ_{12} term, which violates softly this symmetry, since it will play a special role in our calculation of radiative corrections and it is required in order to get the decoupling limit of the model [23]. Similarly, we will use the full Higgs potential Eq. (20) because the λ_6 and λ_7 parameters will induce important corrections to the self scalar couplings [24, 25]. This model is called 2HDM-III, it includes two neutral scalar fields, h and H , and h is the lightest Higgs boson associated to the SM. This model predicts also a CP odd scalar A and two charged Higgs bosons H^\pm .

The effective vertex hZZ in the 2HDM includes also the Feynman diagrams shown in Figure 5 and two more that are shown in Figure 6 for the contributions coming from the virtual exchange of charged Higgs bosons. The heavy neutral scalar H also gives a contribution in the diagrams of Figures 4 and 5. Even more, since the Zff 2HDM couplings are the same as in the SM, the invariant decay amplitude is also given by Eq. (4) with the tree-diagram amplitude given by

$$\begin{aligned} |\mathcal{M}|_{tree}^2 &= \frac{-g^4(f_A^2 + f_V^2)s_{\beta-\alpha}^2}{8c_W^4 m_Z^4} \mathcal{K}(s_1, s_2, m_h, m_Z, m_f) \\ &= |\mathcal{M}_{SM}|_{tree}^2 s_{\beta-\alpha}, \end{aligned} \quad (21)$$

where $s_{\beta-\alpha} = \sin(\beta - \alpha)$ and α is the angle that defines the mixing of the two CP-even

scalar bosons. The one-loop amplitude has to include the charged Higgs contribution

$$\begin{aligned}
|\mathcal{M}|_{1-loop}^2 &= \frac{-g^4(f_A^2 + f_V^2)\mathcal{G}_1^2|\mathcal{F}^g|^2}{8c_W^4 m_Z^4} \mathcal{K}(s_1, s_2, m_\phi, m_Z, m_f) \\
&= \frac{-g^4(f_A^2 + f_V^2)}{8c_W^4 m_Z^4} \left(\frac{g^2 c_W}{128\pi^2 k_s^8 m_Z} \right)^2 \mathcal{K}(s_1, s_2, m_h, m_Z, m_f) \\
&\quad \times |\mathcal{F}_f^g + \mathcal{F}_W^g + \mathcal{F}_S^g + \mathcal{F}_{3\phi}^g + \mathcal{F}_{H^+}^g|^2,
\end{aligned} \tag{22}$$

were the function $\mathcal{F}_{H^\pm}^g$ represents the contribution from the charged Higgs boson and are included in the Appendix. The functions \mathcal{F}_S^g and $\mathcal{F}_{3\phi}^g$ include also the contribution coming from the heavy neutral Higgs boson H while the functions \mathcal{F}_f^g and \mathcal{F}_W^g include a dependence with the mixing angles $\beta - \alpha$. The invariant amplitude for the interference contribution is now given by

$$\begin{aligned}
\mathcal{M}_{int} &= \frac{-g^4(f_A^2 + f_V^2)s_{\beta-\alpha}^2}{4c_W^4 m_Z^4} \left(\frac{g^2 c_W}{128\pi^2 k_s^8 m_Z} \right) \mathcal{K}(s_1, s_2, m_h, m_Z, m_f) \\
&\quad \times \text{Re}[\mathcal{F}_f^g + \mathcal{F}_W^g + \mathcal{F}_S^g + \mathcal{F}_{3\phi}^g + \mathcal{F}_{H^+}^g],
\end{aligned} \tag{23}$$

and the 2HDM integrated decay width can be expressed by

$$\begin{aligned}
\Gamma(h \rightarrow Zll) &= \frac{m_h}{256\pi^3} \left(\frac{-g^4(f_A^2 + f_V^2)}{8c_W^2 m_Z^4} \right) \int_{x_{1i}}^{x_{1f}} \int_{x_{2i}}^{x_{2f}} \mathcal{K}(s_1, s_2, m_h, m_Z, m_f) \left[s_{\beta-\alpha}^2 \right. \\
&\quad + \frac{2g^2 c_W s_{\beta-\alpha}}{128\pi^2 k_s^8 m_Z} \text{Re}[\mathcal{F}_f^g + \mathcal{F}_W^g + \mathcal{F}_S^g + \mathcal{F}_{3\phi}^g \mathcal{F}_{H^+}^g] \\
&\quad \left. + \left(\frac{g^2 c_W s_{\beta-\alpha}}{128\pi^2 k_s^8 m_Z} \right)^2 |\mathcal{F}_f^g + \mathcal{F}_W^g + \mathcal{F}_S^g + \mathcal{F}_{3\phi}^g \mathcal{F}_{H^+}^g|^2 \right] dx_2 dx_1.
\end{aligned} \tag{24}$$

IV. DISCUSSION AND CONCLUDING REMARKS

In order to determine the sensitivity of the decay width of $h \rightarrow ZZ^* \rightarrow Zl^+l^-$ to the hhh coupling, we will find convenient to define the rate R ,

$$\begin{aligned}
R &= \frac{\sigma(gg \rightarrow h) \times \text{Br}(h \rightarrow ZZ^* \rightarrow Zl^+l^-)}{\sigma(gg \rightarrow h_{SM}) \times \text{Br}(h_{SM} \rightarrow ZZ^* \rightarrow Zl^+l^-)_{tree}} \\
&\approx \mathcal{G}_{htt}^2 \frac{\text{Br}(h \rightarrow ZZ^* \rightarrow Zl^+l^-)}{\text{Br}(h_{SM} \rightarrow ZZ^* \rightarrow Zl^+l^-)_{tree}},
\end{aligned} \tag{25}$$

where the factor $\mathcal{G}_{htt} = 1$ for the SM and it varies for each type of 2HDM. In the Appendix we include the respective expressions of each 2HDM contribution. It is important to stress that the main difference in calculating the rate R lies in the production cross section for each

Sector	$R_{SM} = BR_{1-loop}/BR_{tree}$
total	0.994
Yukawa	1.0002
Gauge	0.999
Scalar (not hhh)	.999
hhh coupling	0.996

TABLE I: The contributions of every sector to rate R_{SM} at one loop level.

model that receives a dominant contribution from the top-quark one-loop Feynman diagram. This contribution is contained in the \mathcal{G}_{htt} factor included in Eq. (25).

We analyze first the behavior of the SM contributions associated to the tree- and one-level Feynman diagrams with $\mathcal{G}_{htt} = 1$ in Eq (25) and

$$R_{SM} = \frac{Br(h \rightarrow ZZ^* \rightarrow Zl^+l^-)}{Br(h_{SM} \rightarrow ZZ^* \rightarrow Zl^+l^-)_{tree}}. \quad (26)$$

In Table I are depicted the respective contributions coming from each sector of Feynman diagrams. The total one-loop correction to the SM rate is below the 1% level in agreement with previous results. However, the rate R_{SM} is sensitive to the value used for the SM hhh coupling and in Figure 7 we present the dependence of this rate with respect to the normalized coupling lambda in the range $-3 < \lambda < +3$. We can appreciate that now the radiative correction to the SM rate R_{SM} may be as high as 4% with respect to the tree-level result. A similar correction will be obtained for the 2HDM model.

The 2HDM presents strong modifications for the Higgs self coupling: it is rather sensitive to the mixing angles and other couplings. This is the reason for presenting our results for the radiative corrections in three versions of the 2HDM: with \mathcal{Z}_2 exact symmetry, with only soft violations of the \mathcal{Z}_2 symmetry, and for the most general 2HDM. We present in Figure 8 the dependence of the normalized coupling λ with respect to $\tan \beta$ and m_{H^+} . There is a strong dependence of λ for each of the three 2HDM parameters, with typical increases of order $\lambda \sim 4$.

In Table II we depict the respective contributions coming from the radiative corrections induced on R_{2HDM} by the different sectors of the 2HDM with \mathcal{Z}_2 symmetry. The enhance-

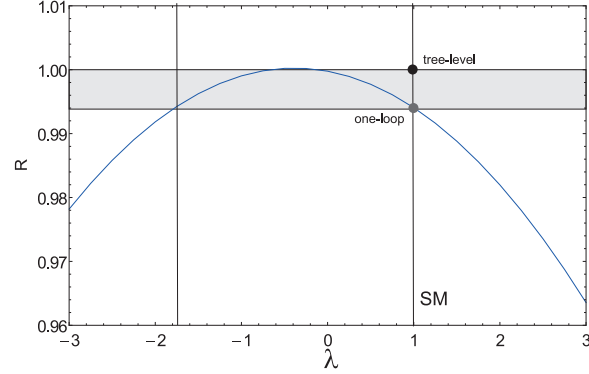


FIG. 7: Behavior of the ratio R with respect to $\lambda = \lambda_{NP}/\lambda_{SM}$. The SM value at tree level is represented by a black point and the SM at one loop level is represented by grey point.

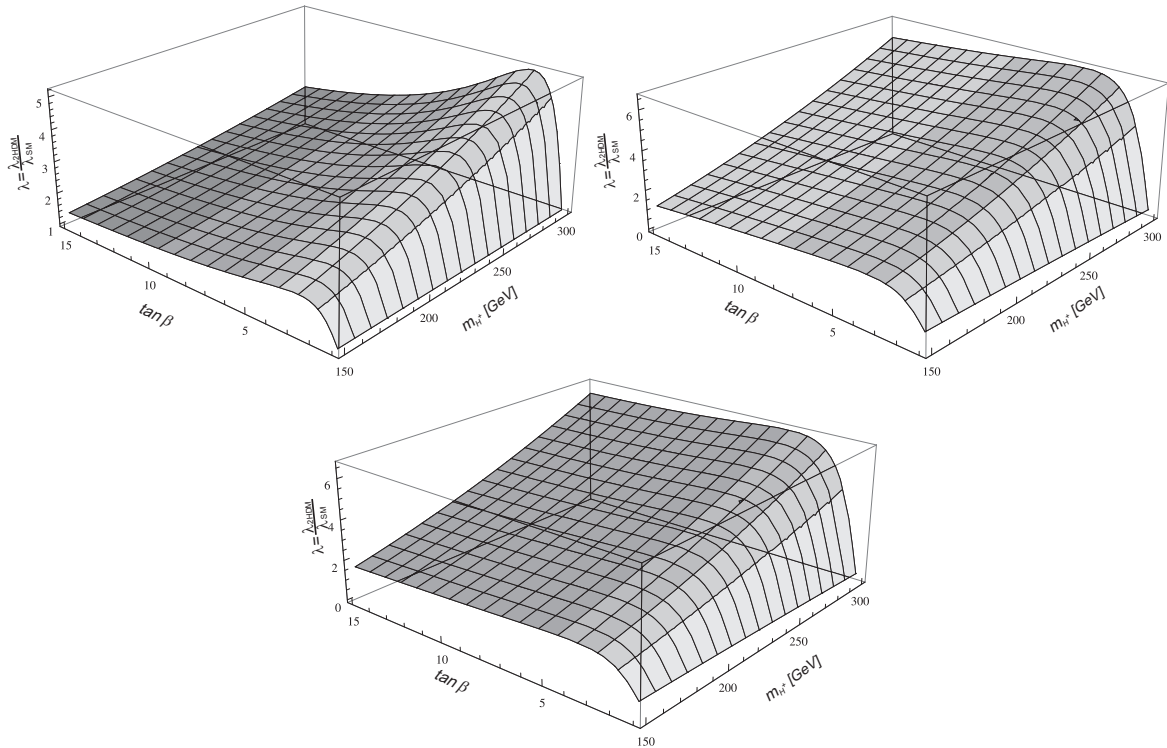


FIG. 8: Behavior of lambda ($\lambda = \lambda_{2HDM}/\lambda_{SM}$) around of SM-like scenario ($\beta - \alpha \approx \pi/2$, $\delta = -0.1$): a) 2HDM with \mathcal{Z}_2 strict symmetry, b) 2HDM with soft \mathcal{Z}_2 symmetry ($\mu_{12} = 200$ GeV), c) 2HDM without imposed symmetry ($\mu_{12} = 200$ GeV, $\lambda_6 = \lambda_7 = 1$).

ment of the Rate R_{2HDM} can as high as 4%. The main difference with respect to the SM result comes from the charged Higgs loops and the neutral Higgs bosons H and A . Accordingly, the enhancement could be even larger in the other two versions of the 2HDM, of order 30% due to the weak limits imposed by the LHC data on the mixing angles and masses of

Sector	$R = BR_{1-loop}^{2HDM-I} / BR_{tree}^{SM}$	$R = BR_{1-loop}^{2HDM-I} / BR_{tree}^{SM}$	$R = BR_{1-loop}^{2HDM-II} / BR_{tree}^{SM}$
total	0.961	0.885	0.682
Yukawa	0.985	0.987	0.775
Gauge	0.984	0.987	0.774
Scalar (not $\phi\phi\phi$)	0.984	0.986	0.775
Higgs charged	0.985	0.987	0.775
triple Higgs	0.966	0.896	0.692

TABLE II: The contributions of every sector to the rate R_{2HDM} with \mathcal{Z}_2 symmetry. The first column represents 2HDM-I with $m_{H^+} = 150 \text{ GeV}$, $\tan\beta = 5$ and $\alpha = \beta - \pi/2 - 0.1$, the second column is for 2HDM-I with $m_{H^+} = 350 \text{ GeV}$, $\tan\beta = 5$ and $\alpha = \beta - \pi/2 - 0.1$ and the third column represent the 2HDM-II with $m_{H^+} = 150 \text{ GeV}$, $\tan\beta = 5$ and $\alpha = \beta - \pi/2 - 0.01$.

the extra Higgs bosons as it is shown in Figures 9 and 10. This flexibility induces a large radiative correction to the rate R_{2HDM} via the corrected triple Higgs bosons couplings of these models.

In conclusion, we have presented the sensitivity expected in the decay rate of the Higgs decay $h \rightarrow ZZ^* \rightarrow Zl^+l^-$ to the radiative corrections induced by the triple Higgs boson coupling shown in Figures 5 and 6. While in the SM this effect is below the 1% level, there could be an enhancement of one order of magnitude if the hhh coupling differs from the SM expectation of the Higgs self coupling. On the other hand, in the three versions studied of the 2HDM, we have found that the radiative corrections to the Higgs decay rate could be much larger due to the weak limits imposed to the mixing angles and masses of the new Higgs bosons. In the latter case, a new window could be opened to test the predictions of the 2HDM if the Higgs decay width could be measured with an accuracy below the 5% level.

ACKNOWLEDGMENTS

We appreciate the support from CONACyT (Mexico) and useful discussions with F. Larios.

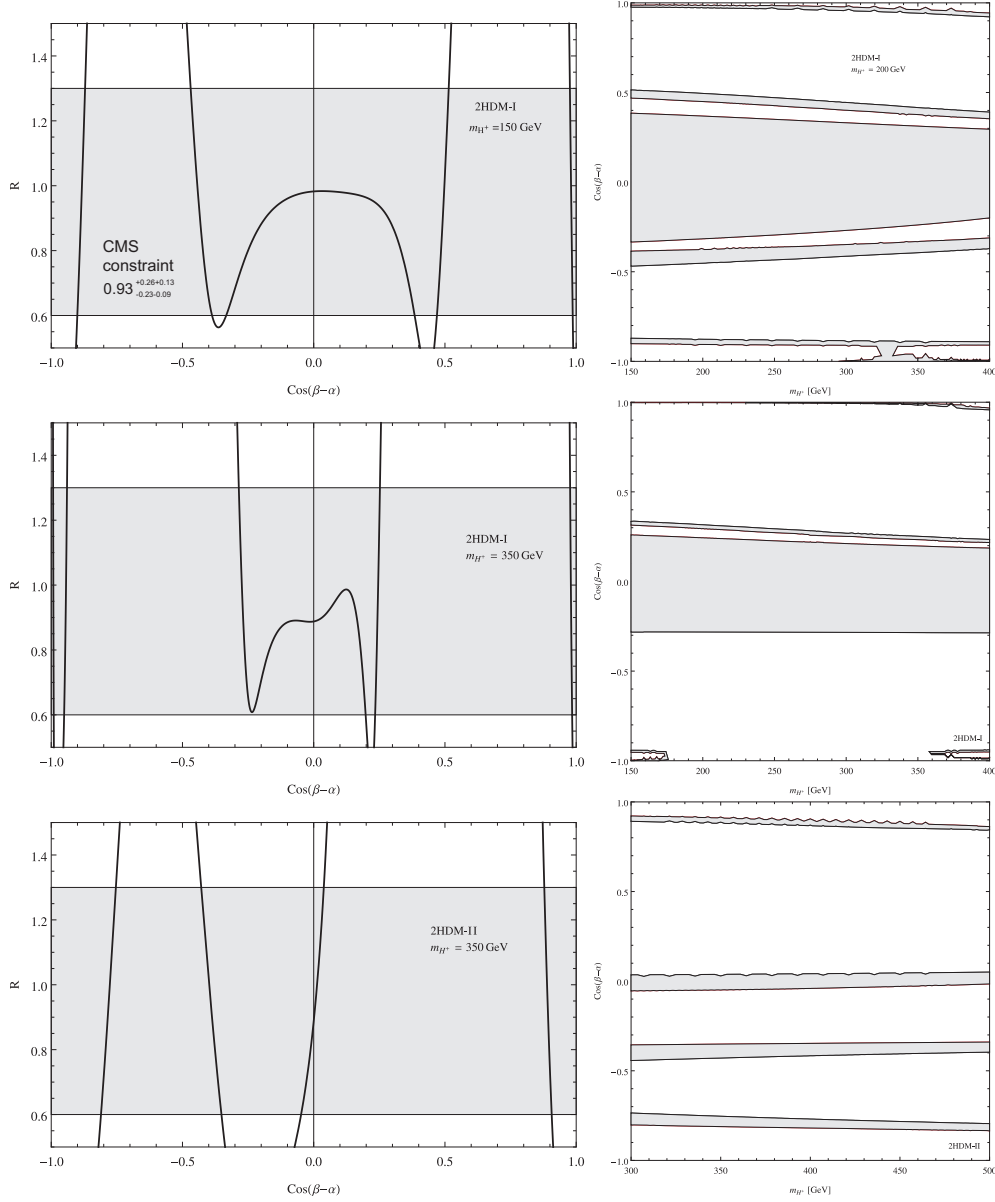


FIG. 9: The grey areas correspond to the allowed regions imposed to the rate R by the LHC on the 2HDM mixing angles and the charged Higgs boson mass [26]. In the left plots, we depict the variation of R with respect to the two types of 2HDM with \mathcal{Z}_2 symmetry and the right plots we include the respective constrains used in the $m_{H^+} - \cos(\beta - \alpha)$ space.

Appendix

We have used in our calculations the Feynman rules corresponding to the 2HDM-III which are given in detail in Refs. [24, 25]. The gauge boson vector couplings were used in the unitary gauge and the respective Yukawa couplings are determined by the four zeros

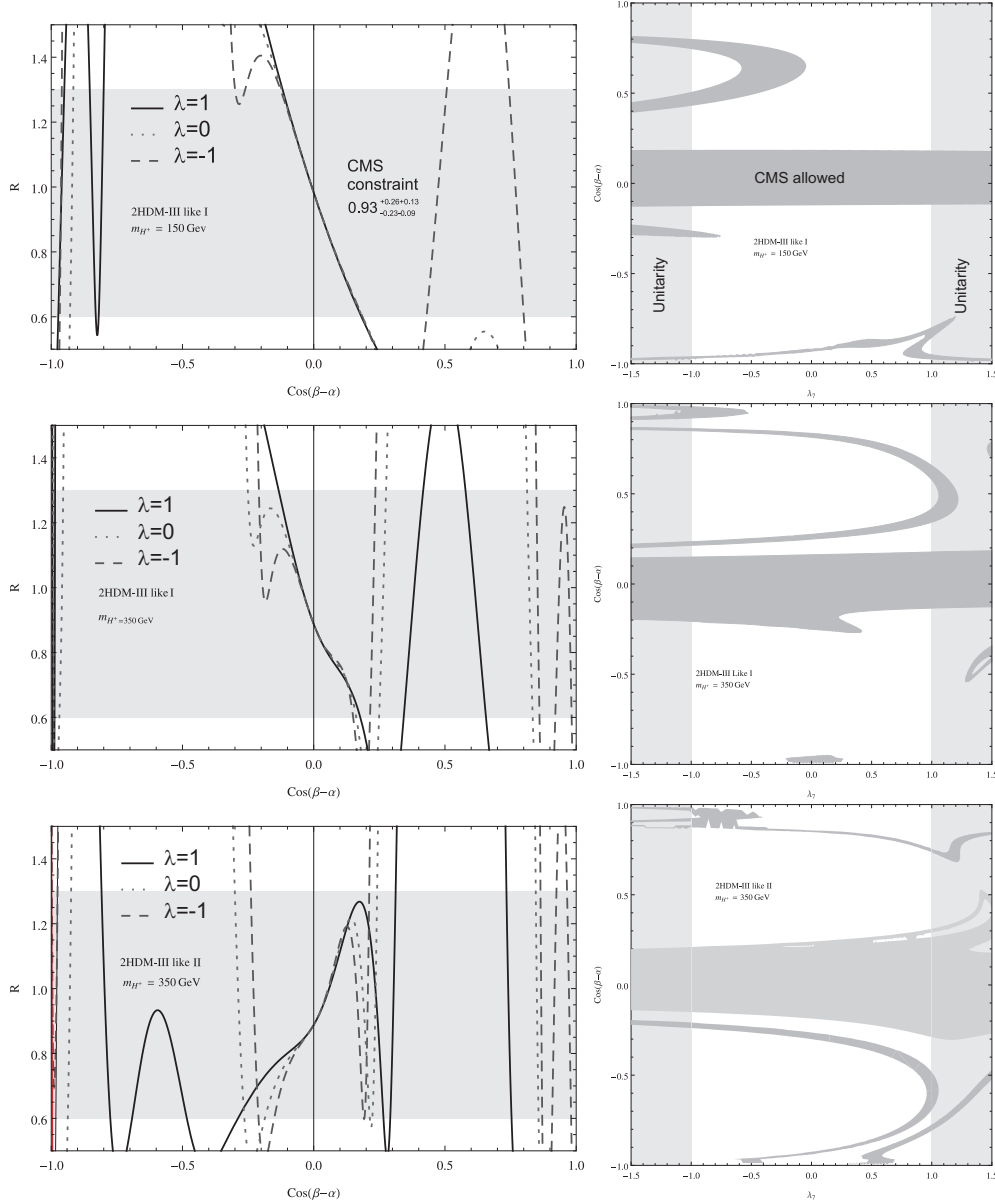


FIG. 10: The grey areas correspond to the allowed regions imposed to the rate R by the LHC on the 2HDM mixing angles and the charged Higgs boson mass [26]. In the left plots, we depict the variation of R with respect to the two types of parametrizations for the 2HDM-III and the right plots we include the respective constraints used in the $m_{H^+} - \cos(\beta - \alpha)$ space.

texture version of 2HDM [27]. The respective factors $\mathcal{G}_{\phi f f}$, $\mathcal{G}_{h W W}$ and $\mathcal{G}_{h \phi_i \phi_j}$ required for the one-loop calculations are depicted in Tables III and IV.

We include below also the explicit expressions for the one-loop contributions obtained for the fermion loops (Figure 2), the W boson loops (Figure 3), the scalar- Z boson loops

\mathcal{G}_{hff}	ll	dd	uu
2HDM-III Like I	$\frac{c_\alpha}{s_\beta} + \frac{\chi_{ll}c_{\beta-\alpha}}{\sqrt{2}s_\beta}$	$\frac{c_\alpha}{s_\beta} + \frac{\chi_{dd}c_{\beta-\alpha}}{\sqrt{2}s_\beta}$	$\frac{c_\alpha}{s_\beta} - \frac{\chi_{uu}c_{\beta-\alpha}}{\sqrt{2}s_\beta}$
2HDM-III Like II	$\frac{-s_\alpha}{c_\beta} + \frac{\chi_{ll}c_{\beta-\alpha}}{\sqrt{2}c_\beta}$	$\frac{-s_\alpha}{c_\beta} + \frac{\chi_{dd}c_{\beta-\alpha}}{\sqrt{2}c_\beta}$	$\frac{c_\alpha}{s_\beta} - \frac{\chi_{uu}c_{\beta-\alpha}}{\sqrt{2}s_\beta}$

TABLE III: Yukawa couplings for the neutral Higgs boson h in the 2HDM-III. The particular cases for SM and $2HDM$ with \mathcal{Z}_2 symmetry are achieved when $\beta - \alpha = \pi/2$, or $\chi_{ff} = 0$, respectively.

Factor coupling	Factor function
$\mathcal{G}_{hH^+H^-}$	$\frac{-1}{16g^2m_W^2} \left\{ 16g^2\mu_{12}^2 \frac{c_{\alpha+\beta}}{s_{2\beta}^2} - 2g^2m_h^2 \frac{c_{\alpha-3\beta+3c_{\alpha+\beta}}}{s_{2\beta}} - 8m_W^2\lambda_6 \frac{c_{\alpha-\beta}}{s_\beta^2} + 8m_W^2\lambda_7 \frac{c_{\alpha-\beta}}{c_\beta^2} \right.$ $\left. + \frac{g^2m_{H^+}^2}{c_\beta} \left(s_{\alpha-2\beta} + 3s_{2\alpha-\beta} - s_{\alpha+2\beta} + s_{2\alpha+3\beta} - s_{\alpha+4\beta} + s_\alpha - 3s_\beta + s_{3\beta} \right) \right\}$
\mathcal{G}_{hhh}	$2m_h^2 \frac{(c_{3\alpha-\beta+3c_{\alpha+\beta}})}{s_{2\beta}} + 2m_{H^+}^2 s_{2\alpha} \frac{(-c_{2\alpha+\beta}+c_{\alpha+2\beta}+c_{\alpha-c_\beta})}{c_\beta} - 16\mu_{12}^2 \frac{c_{\alpha+\beta}c_{\alpha-\beta}^2}{s_{2\beta}^2}$ $+ 8m_W^2\lambda_6 \frac{c_{\alpha-\beta}^3}{g^2s_\beta^2} - 8m_W^2\lambda_7 \frac{c_{\alpha-\beta}^3}{g^2c_\beta^2}$
\mathcal{G}_{hhH}	$\frac{1}{3} \left\{ 4m_H^2 s_{2\alpha} \frac{c_{\alpha-\beta}}{s_{2\beta}} + 8m_h^2 s_{2\alpha} \frac{c_{\alpha-\beta}}{s_{2\beta}} + 2m_{H^+}^2 \frac{(c_\alpha-c_\beta)(c_{\beta-\alpha}+3c_{3\alpha+\beta})}{c_\beta} \right.$ $\left. - 4\mu_{12}^2 \frac{(s_{\alpha-3\beta}+3s_{3\alpha-\beta}+2s_{\alpha+\beta})}{s_{2\beta}^2} + 24m_W^2\lambda_6 \frac{s_{\alpha-\beta}c_{\alpha-\beta}^2}{g^2s_\beta^2} - 24m_W^2\lambda_7 \frac{s_{\alpha-\beta}c_{\alpha-\beta}^2}{g^2c_\beta^2} \right.$
\mathcal{G}_{hHH}	$\frac{1}{3} \left\{ 4m_h^2 s_{2\alpha} \frac{s_{\alpha-\beta}}{s_{2\beta}} + 8m_H^2 s_{2\alpha} \frac{s_{\alpha-\beta}}{s_{2\beta}} + 2m_{H^+}^2 \frac{(c_\alpha-c_\beta)(s_{\beta-\alpha}+3s_{3\alpha+\beta})}{c_\beta} \right.$ $\left. - 4\mu_{12}^2 \frac{(c_{\alpha-3\beta}-3c_{3\alpha-\beta}+2c_{\alpha+\beta})}{s_{2\beta}^2} + 24m_W^2\lambda_6 \frac{s_{\alpha-\beta}^2c_{\alpha-\beta}}{g^2s_\beta^2} - 24m_W^2\lambda_7 \frac{s_{\alpha-\beta}^2c_{\alpha-\beta}}{g^2c_\beta^2} \right.$
\mathcal{G}_{hWW}	$s_{\beta-\alpha}$
\mathcal{G}_{HWW}	$c_{\beta-\alpha}$

TABLE IV: Scalar and vector boson couplings in the 2HDM-III.

(Figure 4) and the charged and neutral Higgs boson loops (Figures 5 and 6).

Contribution for the fermion loop (Figure 2):

$$\begin{aligned}
\mathcal{F}_f^g = & \sum_f \frac{-N_c^f m_f^2 \mathcal{G}_{hff}}{c_W^2 m_W} \left\{ k_s^8 (f_A^2 + f_V^2) + k_s^4 \left(k_1^2 \left[(f_A^2 + f_V^2) [k_1 \cdot k_2]^2 + k_s^4 (f_A^2 - f_V^2) \right] \right. \right. \\
& - 2k_s^4 \left[m_f^2 (f_A^2 - f_V^2) + f_V^2 k_1 \cdot k_2 \right] + (f_A^2 + f_V^2) [k_1 \cdot k_2]^3 \Big) C_0(k_1, k_2) \\
& + k_s^4 \left((f_A^2 + f_V^2) k_1 \cdot k_2 [k_1^2 + k_1 \cdot k_2] + k_s^4 f_V^2 \right) B_0(p, k_1) \\
& \left. - k_s^8 f_A^2 \left(B_\mu(k_1, \mu) + B_\mu(p, \mu) \right) \right\} + \{k_1 \leftrightarrow k_2\}, \tag{27}
\end{aligned}$$

the f_A and f_V represent the axial and vectorial contribution, respectively. On the other

hand, we have introduced a short notation for the Passarino-Veltman functions

$$C_0(k_i, k_j) = C_0(k_i^2, k_j^2, (k_i + k_j)^2, m^2, m^2, m^2), \quad (28)$$

$$B_0(k_i, k_j) = B_0(k_i^2, m^2, m^2) - B_0(k_j^2, m^2, m^2), \quad (29)$$

$$B_\mu(k_i, \mu_R) = B_0(k_i, m^2 + \mu_R^2, m^2 + \mu_R^2) - B_0(0, \mu_R^2, \mu_R^2), \quad (30)$$

where $B_0(k_i, k_j)$ is a finite contribution, and $B_\mu(k_i, \mu_R)$ is a renormalized contribution [28].

Contribution for the W -boson loop (Figure 3):

$$\begin{aligned} \mathcal{F}_W^g = & \frac{c_W^2 \mathcal{G}_{hWW}}{9m_W^5} \left(2k_s^8 \left\{ -18k_1^4 m_W^2 + k_1^2 (-36m_W^2 k_1 \cdot k_2 + 11[k_1 \cdot k_2]^2 - 11k_s^4) \right. \right. \\ & -9(k_s^4 - 4m_W^2) k_1 \cdot k_2 - 31m_W^2 [k_1 \cdot k_2]^2 + 9[k_1 \cdot k_2]^3 + 31k_s^4 m_W^2 + 108m_W^6 \left. \right\} \\ & +9k_s^4 \left\{ 2k_1^6 m_W^2 (k_s^4 - [k_1 \cdot k_2]^2) + k_1^4 \left[-2k_s^4 (k_1 \cdot k_2 - 2m_W^2)^2 \right. \right. \\ & + [k_1 \cdot k_2]^3 (k_1 \cdot k_2 - 8m_W^2) + k_s^8 \left. \right] + 4k_1^2 \left[-2(k_s^4 - m_W^4) [k_1 \cdot k_2]^3 \right. \\ & + 3m_W^2 (k_s^4 + 2m_W^4) [k_1 \cdot k_2]^2 + k_s^4 (k_s^4 + 2m_W^4) k_1 \cdot k_2 - 3m_W^2 [k_1 \cdot k_2]^4 \\ & + [k_1 \cdot k_2]^5 - 6k_s^4 m_W^6 \left. \right] - k_s^8 (2m_W^2 k_1 \cdot k_2 - 5[k_1 \cdot k_2]^2 + 12m_W^4) \\ & + k_s^4 (-72m_W^6 k_1 \cdot k_2 + 4m_W^4 [k_1 \cdot k_2]^2 + 8m_W^2 [k_1 \cdot k_2]^3 - 7[k_1 \cdot k_2]^4 + 48m_W^8) \\ & + [k_1 \cdot k_2]^3 (8m_W^4 k_1 \cdot k_2 - 6m_W^2 [k_1 \cdot k_2]^2 + 3[k_1 \cdot k_2]^3 + 24m_W^6) - k_s^{12} \left. \right\} C_0(k_1, k_2) \\ & -12k_s^8 m_W^2 (k_s^4 - 4k_2^2 m_W^2) B_0(k_1, 0) - 9k_s^4 \left\{ k_1^4 (-k_s^4 k_1 \cdot k_2 - 6m_W^2 [k_1 \cdot k_2]^2 \right. \\ & + [k_1 \cdot k_2]^3 + 2k_s^4 m_W^2) + [k_1 \cdot k_2]^3 (-6k_2^2 m_W^2 - 4k_s^4 + 8m_W^4) \\ & + [k_1 \cdot k_2]^2 [4m_W^2 (k_s^4 + 6m_W^4) - 2k_2^2 (k_2^2 m_W^2 + k_s^4)] \\ & + k_1^2 k_1 \cdot k_2 [k_1 \cdot k_2 (3k_1 \cdot k_2 (k_1 \cdot k_2 - 2m_W^2) - 2k_s^4 + 8m_W^4) + 6m_W^2 (k_s^4 + 4m_W^4)] \\ & + k_s^4 k_1 \cdot k_2 (6k_2^2 m_W^2 + k_s^4 - 8m_W^4) + (k_2^2 - 6m_W^2) [k_1 \cdot k_2]^4 - 2k_1^6 m_W^2 k_1 \cdot k_2 \\ & + 3[k_1 \cdot k_2]^5 + 2k_s^4 m_W^2 (k_2^4 - 12m_W^4) \left. \right\} B_0(k_1, p) + 12k_s^8 m_W^2 [k_1 \cdot k_2]^2 B_0(p, 0) \\ & -3k_s^8 \left\{ 6k_s^4 k_1 \cdot k_2 + k_1^2 (5k_s^4 - 8[k_1 \cdot k_2]^2) - 6[k_1 \cdot k_2]^3 + k_s^4 (3k_2^2 + 2m_W^2) \right\} B_\mu(k_1, \mu) \\ & + 6k_s^8 m_W^2 (7[k_1 \cdot k_2]^2 - 6k_s^4) B_\mu(p, \mu) \left. \right) + \{k_1 \leftrightarrow k_2\}, \quad (31) \end{aligned}$$

here we have used the same definition for PV-functions expressed in (28,29) and (30). The SM case is achieved when $\mathcal{G}_{hWW} = 1$.

Contribution for the charged Higgs boson loops (Figure 6):

$$\begin{aligned}
\mathcal{F}_{H^\pm}^g &= \frac{4g\mathcal{G}_{hH^+H^-}m_W c_{2W}^2}{c_W^2} \left\{ k_s^4 + \left[k_s^4(-k_s^4 k_1 \cdot k_2 + [k_1 \cdot k_2]^3 + 2k_s^4 m_{H^+}^2) \right. \right. \\
&\quad \left. \left. + k_1^2 k_s^4 ([k_1 \cdot k_2]^2 - k_s^4) \right] C_0(k_1, k_2) + k_s^4 (-[k_1 \cdot k_2]^2 - k_1^2 k_1 \cdot k_2 + k_s^4) B_0(k_1, p) \right\} \\
&\quad + \{k_1 \leftrightarrow k_2\}, \tag{32}
\end{aligned}$$

for the SM case this form factor is equal to zero.

Contribution for the scalar- Z boson loops (Figure 4):

$$\begin{aligned}
\mathcal{F}_S^g &= \sum_{i=h,H} \frac{k_s^4 \mathcal{G}_{\phi_i WW}}{9c_W^3 m_Z (k_s^4 - [k_1 \cdot k_2]^2)} \left\{ \mathcal{G}_{\phi_i WW} \mathcal{G}_{hWW} \left[2k_1^2 k_s^4 [11(k_s^4 - [k_1 \cdot k_2]^2) \right. \right. \\
&\quad \left. \left. + 3(m_{\phi_i}^2 - m_Z^2)^2 - 18k_s^4 (k_s^4 - [k_1 \cdot k_2]^2) (m_{\phi_i}^2 - k_1 \cdot k_2) \right] \right. \\
&\quad \left. + \delta_{hi} \left[-k_1^2 k_s^4 [2(k_s^4 - [k_1 \cdot k_2]^2) - 3(m_{\phi_i}^2 - m_Z^2)^2] + 9k_s^4 (k_s^4 - [k_1 \cdot k_2]^2) (m_{\phi_i}^2 + m_Z^2) \right] \right. \\
&\quad \left. + 9C_0(k_1^2, k_2^2, p^2, m_Z^2, m_{\phi_i}^2, m_Z^2) \mathcal{G}_{\phi_i WW} \mathcal{G}_{hWW} (k_s^4 - [k_1 \cdot k_2]^2) \left[k_1^4 [2(m_{\phi_i}^2 - m_Z^2) k_1 \cdot k_2 \right. \right. \\
&\quad \left. \left. + [k_1 \cdot k_2]^2 - k_s^4 + (m_{\phi_i}^2 - m_Z^2)^2 \right] + 2k_1^2 [-2k_1 \cdot k_2 (k_s^4 - m_{\phi_i}^4 + m_{\phi_i}^2 m_Z^2) \right. \\
&\quad \left. + (4m_{\phi_i}^2 - 3m_Z^2) [k_1 \cdot k_2]^2 + 2[k_1 \cdot k_2]^3 + m_Z^2 (k_s^4 + (m_{\phi_i}^2 - m_Z^2)^2) \right] + 2k_1 \cdot k_2 [(m_Z^3 - m_{\phi_i}^2 m_Z)^2 \\
&\quad - k_s^4 (m_{\phi_i}^2 - 2m_Z^2)] - [k_1 \cdot k_2]^2 (4k_s^4 - 3m_{\phi_i}^4 + 2m_{\phi_i}^2 m_Z^2 + m_Z^4) + 2(3m_{\phi_i}^2 - 2m_Z^2) [k_1 \cdot k_2]^3 \\
&\quad \left. + 3[k_1 \cdot k_2]^4 + k_s^4 (k_s^4 - m_{\phi_i}^4 + 2m_{\phi_i}^2 m_Z^2 - 5m_Z^4) \right] + [B_0(k_1^2, m_{\phi_i}^2, m_Z^2) - B_0(p^2, m_Z^2, m_Z^2)] \\
&\quad \times 3\mathcal{G}_{\phi_i WW} \mathcal{G}_{hWW} \left[3k_1^4 ([k_1 \cdot k_2]^2 - k_s^4) (k_1 \cdot k_2 + m_{\phi_i}^2 - m_Z^2) + k_1^2 [-3m_Z^2 ([k_1 \cdot k_2]^2 - k_s^4) \right. \\
&\quad \left. \times (k_1 \cdot k_2 - 2m_{\phi_i}^2) + 6m_Z^4 (k_s^4 - [k_1 \cdot k_2]^2) + 3k_1 \cdot k_2 (3[k_1 \cdot k_2]^3 + 3[k_1 \cdot k_2]^2 m_{\phi_i}^2 - 2k_1 \cdot k_2 k_s^4 \right. \\
&\quad \left. - 3k_s^4 m_{\phi_i}^2) \right] - m_Z^2 ([k_1 \cdot k_2]^2 - k_s^4) [3k_1 \cdot k_2 (k_1 \cdot k_2 - 2m_{\phi_i}^2) - k_s^4] + 6k_1 \cdot k_2 m_Z^4 (k_s^4 - [k_1 \cdot k_2]^2) \\
&\quad \left. + k_1 \cdot k_2 [k_1 \cdot k_2 m_{\phi_i}^2 (9[k_1 \cdot k_2]^2 - 8k_s^4) + 3(3[k_1 \cdot k_2]^4 - 4[k_1 \cdot k_2]^2 k_s^4 + k_s^8)] \right. \\
&\quad \left. + 3k_1 \cdot k_2 k_2^2 ([k_1 \cdot k_2]^3 + [k_1 \cdot k_2]^2 (m_{\phi_i}^2 - m_Z^2) - 2k_1 \cdot k_2 k_s^4 + k_s^4 (m_Z^2 - m_{\phi_i}^2)) \right] \\
&\quad + [B_0(k_1^2, m_{\phi_i}^2, m_Z^2) - B_0(0, m_Z^2, m_Z^2)] \times 3k_2^2 k_s^4 m_Z^2 (m_{\phi_i}^2 - m_Z^2) (2\mathcal{G}_{\phi_i WW} \mathcal{G}_{hWW} - \delta_{hi}) \\
&\quad - [B_0(k_1^2, m_{\phi_i}^2, m_Z^2) - B_0(0, m_{\phi_i}^2, m_{\phi_i}^2)] \times 3k_2^2 k_s^4 m_{\phi_i}^2 (m_{\phi_i}^2 - m_Z^2) (2\mathcal{G}_{\phi_i WW} \mathcal{G}_{hWW} - \delta_{0h}) \\
&\quad + [B_0(p^2, m_Z^2, m_Z^2) - B_0(0, m_Z^2, m_Z^2)] \times 6\mathcal{G}_{\phi_i WW} \mathcal{G}_{hWW} k_s^4 m_Z^2 (k_s^4 - [k_1 \cdot k_2]^2) \\
&\quad - [B_0(p^2, m_Z^2, m_Z^2) - B_0(0, m_{\phi_i}^2, m_{\phi_i}^2)] \times 6\mathcal{G}_{\phi_i WW} \mathcal{G}_{hWW} k_s^4 m_{\phi_i}^2 [k_1 \cdot k_2]^2 \\
&\quad + k_s^4 B_{k_1 \mu R}(m_{\phi_i}) \left[3k_1^2 (\mathcal{G}_{\phi_i WW} \mathcal{G}_{hWW} (5k_s^4 - 8[k_1 \cdot k_2]^2) + \delta_{hi} ([k_1 \cdot k_2]^2 - k_s^4)) \right. \\
&\quad \left. - 3(\mathcal{G}_{\phi_i WW} \mathcal{G}_{hWW} (6[k_1 \cdot k_2]^3 - 6k_1 \cdot k_2 k_s^4 + k_s^4 m_{\phi_i}^2) + 2\delta_{hi} ([k_1 \cdot k_2]^2 - k_s^4) (m_{\phi_i}^2 - 5m_Z^2)) \right]
\end{aligned}$$

$$\begin{aligned}
& +9\mathcal{G}_{\phi_i WW}\mathcal{G}_{hWW}k_2^2k_s^4] + 3k_s^4m_Z^2\delta_{hi}(k_s^4 - [k_1 \cdot k_2]^2)B_{0\mu_R}(m_Z) \\
& -3k_s^4m_{\phi_i}^2[k_s^4(2\mathcal{G}_{\phi_i WW}\mathcal{G}_{hWW} - \delta_{hi}) + [k_1 \cdot k_2]^2\delta_{hi}]B_{0\mu_R}(m_{\phi_i}) \\
& +3\mathcal{G}_{\phi_i WW}\mathcal{G}_{hWW}k_s^4m_{\phi_i}^2(2[k_1 \cdot k_2]^2 - 3k_s^4)B_{p\mu_R}(m_Z)\} + \{k_1 \leftrightarrow k_2\}, \tag{33}
\end{aligned}$$

here we have used a new definitions for the renormalizable PV-functions

$$\begin{aligned}
B_{k_1\mu}(m) &= m_Z^2C_0(k_1^2, 0, k_1^2, m^2 + \mu_R^2, m_Z^2 + \mu_R^2, \mu_R^2) + B_0(k_1^2, \mu_R^2, m^2 + \mu^2) - B_0(0, \mu_R^2, m_Z^2 + \mu_R^2) \\
& + \frac{m_Z^2 + \mu^2}{m_Z^2} \left(B_0(0, m_Z^2 + \mu_R^2, m_Z^2 + \mu_R^2) - B_0(0, \mu_R^2, \mu_R^2) \right) + 1, \tag{34}
\end{aligned}$$

$$B_{p\mu_R}(m) = B_0(p^2, m^2 + \mu_R^2, m^2 + \mu_R^2) - B_0(0, \mu_R^2, \mu_R^2), \tag{35}$$

$$B_{0\mu_R}(m) = B_0(0, m^2 + \mu_R^2, m^2 + \mu_R^2) - B_0(0, \mu_R^2, \mu_R^2). \tag{36}$$

The SM context is attained when $i = h$.

Contribution for the triple Higgs boson loops (Figure 5):

$$\begin{aligned}
\mathcal{F}_{3\phi}^g &= \sum_{i,j=h,H} \frac{3k_s^4\mathcal{G}_{h\phi_i\phi_j}}{2c_W^2m_W} \left\{ \mathcal{G}_{\phi_i WW}\mathcal{G}_{\phi_j WW} \left[2k_s^4 + \left\{ k_1^2 \left(-2(m_{\phi_j}^2 - m_Z^2)k_1 \cdot k_2 + [k_1 \cdot k_2]^2 - k_s^4 \right. \right. \right. \right. \\
& + (m_{\phi_j}^2 - m_Z^2)^2 \left. \left. \left. \left. + k_2^2 \left(-2(m_{\phi_i}^2 - m_Z^2)k_1 \cdot k_2 + [k_1 \cdot k_2]^2 - k_s^4 + (m_{\phi_i}^2 - m_Z^2)^2 \right) \right. \right. \right. \right. \\
& + 2 \left[-k_1 \cdot k_2 \left(k_s^4 + (m_{\phi_i}^2 - m_Z^2)(m_Z^2 - m_{\phi_j}^2) \right) - [k_1 \cdot k_2]^2(m_{\phi_i}^2 + m_{\phi_j}^2 - 2m_Z^2) + [k_1 \cdot k_2]^3 \right. \\
& \left. \left. \left. \left. + k_s^4(m_{\phi_i}^2 + m_{\phi_j}^2 - 4m_Z^2) \right] \right\} C_0(k_1^2, k_2^2, p^2, m_{\phi_i}^2, m_Z^2, m_{\phi_j}^2) + [B_0(k_1^2, m_{\phi_i}^2, m_Z^2) \right. \\
& - B_0(p^2, m_{\phi_i}^2, m_{\phi_j}^2)] \left[k_1^2(m_{\phi_j}^2 - m_Z^2 - k_1 \cdot k_2) - k_1 \cdot k_2(k_1 \cdot k_2 - m_{\phi_i}^2 + m_Z^2) \right] \\
& + [B_0(k_1^2, m_{\phi_j}^2, m_Z^2) - B_0(p^2, m_{\phi_i}^2, m_{\phi_j}^2)] \left[k_1^2(m_{\phi_i}^2 - m_Z^2 - k_1 \cdot k_2) \right. \\
& \left. \left. \left. \left. - k_1 \cdot k_2(k_1 \cdot k_2 - m_{\phi_j}^2 + m_Z^2) \right] \right] + k_s^4 \left[\mathcal{G}_{\phi_i WW}\mathcal{G}_{\phi_j WW} (B_{1\mu_R}(m_{\phi_i}) + B_{1\mu_R}(m_{\phi_j})) \right. \right. \\
& \left. \left. - 2\delta_{ij}B_{p\mu_R}(m_{\phi_i}) \right] \right\} + \{k_1 \leftrightarrow k_2\}, \tag{37}
\end{aligned}$$

the renormalized PV-function have been expressed as Eqs. (34) and (35).

Finally the general tree level decays for the Higgs boson needed for compute the of R factor are given in detail in Ref. [29].

[1] The ATLAS Collaboration, Phys. Lett. B716, 1 (2012) and ATLAS-CONF-2012-162; The CMS Collaboration, Phys. Lett. B716, 30 (2012) and CMS-PAS-HIG-12-045.

- [2] P. Higgs, Phys. Lett. 12, 132 (1964); Phys. Rev. Lett. 13, 508 (1964); F. Englert and R. Brout, Phys. Rev. Lett. 13, 321 (1964); G. Guralnik, C. Hagen and T. Kibble, Phys. Rev. Lett. 13, 585 (1964); S. Weinberg, Phys. Rev Lett. 19, 1264 (1967).
- [3] G.Aad et al. (ATLAS Collaboration, CMS Collaboration), Phys. Rev. Lett. 114, 191803 (2015); Phys. Rev. D91, 012006 (2015); S. Chatrchyar et al.(CMS Collaboration), JHEP 1401, 096 (2014); M. Flechl [ATLAS and CMS Collaborations], J. Phys. Conf. Ser. **631**, no. 1, 012028 (2015) [arXiv:1503.00632 [hep-ex]].
- [4] J.A. Aguilar Saavedra et al., ECFA-DESY LC Physics Working Group Collaboration. hep-ph/0106315.
- [5] A. Gutierrez-Rodriguez, M.A. Hernandez-Ruiz, O.A. Sampayo, Int. J. Mod. Phys. A24, 5299 (2009).
- [6] U. Baur, T. Plehn and D.L. Rainwater, Phys. Rev. D67, 112 (2003); J. Baglio, A. Djouadi, R. Grber, M. M. Mhleitner, J. Quevillon and M. Spira, JHEP **1304** (2013) 151 [arXiv:1212.5581 [hep-ph]].
- [7] A. Djouadi et al., Eur. Phys. J. C10, 45 (1999); S. Dawson, S. Dittmaier and M. Spira, Phys. Rev. D58, 115012 (1998).
- [8] M.J. Dolan, C. Englert, and M. Spannoswsky, JHEP 1210, 112 (2012).
- [9] J. Baglio, A. Djouadi, R. Grber, M. M. Mhleitner, J. Quevillon and M. Spira, JHEP **1304** (2013) 151 [arXiv:1212.5581 [hep-ph]]; J. Baglio, Pos DIS **2014**, 120 (2014) [arXiv:1407.1045 [hep-ph]].
- [10] S. Dawson, A. Ismail and I. Low, Phys. Rev. D **91**, no. 11, 115008 (2015) [arXiv:1504.05596 [hep-ph]].
- [11] F. Maltoni, E. Vryonidou, M. Zaro, arXiv:1408.6542, JHEP 1411, 079 (2014).
- [12] H.J. He, J. Ren and W. Yao, arXiv:1506.03302.
- [13] F. Goertz et al., arXiv:1301.3492, JHEP 1306, 016 (2013).
- [14] M. Flechl [ATLAS and CMS Collaborations], J. Phys. Conf. Ser. **631**, no. 1, 012028 (2015) [arXiv:1503.00632 [hep-ex]].
- [15] R. Martinez, M.A. Perez, J.J. Toscano, Phys.Lett. B340, 91 (1994); F. Larios, R. Martinez, M.A. Perez, Phys. Lett. B345, 259 (1995)
- [16] S. Kanemura, M. Kikuchi and K. Yagyu, Nucl. Phys. B **896**, 80 (2015) [arXiv:1502.07716 [hep-ph]]. S. Kanemura et al., Phys. Lett. B558, 157 (2003)

- [17] S. Heinemeyer *et al.* [LHC Higgs Cross Section Working Group Collaboration], arXiv:1307.1347 [hep-ph].
- [18] Q. H. Cao, Y. Liu and B. Yan, arXiv:1511.03311 [hep-ph].
- [19] A. Arhrib, R. Benbrik, J. El Falaki and A. Jueid, JHEP **1512**, 007 (2015) [arXiv:1507.03630 [hep-ph]].
- [20] H. Castilla-Valdez, C.G. Honorato, A. Moyotl, M.A. Perez (in preparation).
- [21] V. Hankele, G. Klamke, D. Zeppenfeld and T. Figy, Phys. Rev. D **74**, 095001 (2006) [hep-ph/0609075].
- [22] Vernon D. Barger, Roger J. N. Phillips *Collider Physics*,(Addison-Wesley, 1997).
- [23] J.F. Gunion and H.E. Haber, Phys. Rev. D **67**, 075019 (2003).
- [24] J. Hernandez-Sanchez, C. G. Honorato, M. A. Perez and J. J. Toscano, Phys. Rev. D **85**, 015020 (2012) [arXiv:1108.4074 [hep-ph]].
- [25] A. Cordero-Cid, J. Hernandez-Sanchez, C. G. Honorato, S. Moretti, M. A. Perez and A. Rosado, JHEP **1407**, 057 (2014) [arXiv:1312.5614 [hep-ph]].
- [26] S. Chatrchyan *et al.* [CMS Collaboration], arXiv:1312.5353 [hep-ex].
- [27] J. Hernandez-Sanchez, S. Moretti, R. Noriega-Papaqui and A. Rosado, JHEP **1307**, 044 (2013) doi:10.1007/JHEP07(2013)044 [arXiv:1212.6818].
- [28] R. Pittau, JHEP **1211**, 151 (2012) [arXiv:1208.5457 [hep-ph]].
- [29] J.F. Gunion, H.E. Haber, G.L. Kane and S. Dawson, *The Higgs Hunters Guide*, Addison-Wesley, Reading, MA (1990). W.-Y. Keung and W.J. Marciano, Phys. Rev. D **30** (1984). E. Barradas, J.L. Diaz-Cruz, A. Gutierrez and A. Rosado, Phys. Rev. D **53** (1996) 1678. J.L. Diaz-Cruz and M.A. Perez, Phys. Rev. D **33** (1986) 273. M. Gomez-Bock and R. Noriega-Papaqui, J. Phys. G **32** (2006) 761 [hep-ph/0509353].